Investigation of the Properties of Poly Buty-Methacrylate, Polystyrene and their Blends in Order to Create Innovative Solar Cell Encapsulants'

Tyohule Philip Aondongu [*1], Ugwuoke Nnamdi Francis [2], Udie Linus Ugbong [1], and Lekeka Biniam B [3]

[1] Department of Material Science of Semiconductors and Dielectrics, MISIS University, Moscow- Russia

[2] Department of Metallurgical Technology of Non-Ferrous Metals MISIS, Moscow- Russia

[3] Department of Advanced Materials Science, MISIS University, Moscow- Russia

DOI: https://doi.org/10.51584/IJRIAS.2026.11100065

Received: 11 October 2026; Accepted: 16 October 2026; Published: 05 November 2026

ABSTRACT

Solar cell encapsulation represents a critical aspect of solar module design as it serve as a shield to sensitive active layers from environmental degradation, mechanical wear, and chemical instability. Conventional encapsulant materials such as Ethylene Vinyl Acetate (EVA) have been extensively deployed within the solar industry. However, they pose several limitations including susceptibility to UV radiation which eventually leads to yellowing, moisture permeation, thermal instability and mechanical stress. These challenges often impact photovoltaic module performance, reduced module lifespan and increased maintenance costs, thereby hindering the general reliability and economic viability of solar energy technologies. This research therefore investigated Poly Butyl Methacrylate (PBMA), Polystyrene and their blends in respective ratios as advanced encapsulants designed to overcome these challenges. Butyl methacrylate and polystyrene were polymerized using free radical polymerization to obtain poly butyl methacrylate (PBMA) and polystyrene (PS) respectively. The blends were obtained by mixing BMA and PS in the ratio of (25/75)% and (75/25)% of PS:BMA before polymerization. The samples were examined to determine their adhesive properties, optical transparency, resistance to moisture ingress and UV degradation simulating real world scenario. PBMA and (25/75)% blend demonstrated chemical stability, resistance to UV radiation, good optical clarity, and good resistance to moisture ingress. The (75/25)% blend also maintained good adhesion, optical clarity but degraded earlier than PBMA. Pure Polystyrene suffered degradation to UV radiation and weak adhesive properties but showed good strength in moisture resistance. These findings demonstrate that all the polymers but pure polystyrene offer a promising combination of chemical inertness, mechanical robustness and optical performance capable of extending photovoltaic module lifetimes thereby reducing operational costs and enhancing energy yield.

Keywords: Encapsulant, Solar Cells, Polymer, Poly-Butyl Methacrylate, Polystyrene, Degradation

INTRODUCTION

Energy is crucial for societal and economic progress, yet challenges arise from rising oil costs and the environmental impact of fossil fuels. Renewable energy technologies now present viable and dependable alternatives to help meet growing demand and reduce energy shortages. Renewable energy sources such as solar, wind and hydropower offer sustainable answers to global energy needs and related challenges. Photovoltaic(PV) technology in particular has advanced significantly in recent decades with global installations hitting 2.2 terawatts by the end of 2024 amounting to 29 % increase compared to 2023 [31]. Additionally, data from Fraunhofer Laboratory shows that PV module costs have fallen by 25 % with each doubling of manufacturing capacity over the past forty years, a trend driven by technological improvements and production scaling.

A PV module consists of several solar cells connected in series and an array is formed by connecting modules in parallel and series [11]. The overall efficiency of a PV system is directly affected by the power output of the

module, which is dependent on the properties of the solar cells and the immediate surroundings [2].Manufacturers generally claim that photovoltaic (PV) modules have a field lifespan exceeding 25 years with an anticipated annual power loss of about 0,8 % [3, 4]. To verify this, significant experimental research has been carried out to measure degradation rates largely prompted by defects observed in earlier installations such as flaws in solar cells and protective materials. For instance, accelerated stress tests were developed by the National Renewable Energy Laboratory (NREL) to assess module durability and long-term performance [5-7]. Nevertheless, reports persist of abnormal degradation rates caused by various failures which increase operating costs and undermine system reliability. Key factors accelerating degradation include extreme environmental exposure and manufacturing defects [16-18]. When degradation rates are high, PV technology becomes less competitive compared to other renewable energy options [27-28]. Thus, sustained efforts are needed to minimize module degradation, enhance methods for detecting and characterizing defects and improve the accuracy of predicting future performance decline.

Researchers have thoroughly analyzed existing studies and industrial data on photovoltaic (PV) failures, degradation and diagnostic techniques. For instance, classified methods for identifying photovoltaic system failures by physical, environmental and electrical factors were reviewed by Kim and Co [16]. Also, he examined how environmental conditions contribute to module degradation and outlined general detection and prevention strategies. Kim, et al [16] summarized various types of PV module degradation and the accelerated testing procedures used to assess reliability, and R. Heidrich, et al [9] offered a detailed review of degradation and failure modes across all components of PV module design. Despite these thorough analyses, current literature still lacks sufficient coverage of PV degradation and identification methods. This gap emanate from the sudden progress in solar cell technology and the rapid emergence of new and advanced solar cell designs. Consequently, several opportunities remain to improve the dependability of photovoltaic systems through improved research. The encapsulant material is one of the major crux for this PV degradation [19-21, 24-25, 30].

Solar cell is the critical component that converts sunlight into electricity and is the centerpiece of the solar energy revolution [29]. The quantity of sunlight that is converted into electrical power or the efficiency of solar cell is the determinant factor for the general effectiveness of solar power systems. Over the years, the notable improvement in efficiency which directly impacts the level of electrical power generated per unit module has been attributed to serious improvements in solar cell technology. However, photovoltaic cells are not the sole contributor to solar energy's outstanding performance. The success also depends on other factors like the encapsulation layer, which is very important to protect the active layers of the cell by guaranteeing the durability and functionality of the PV modules. Such encapsulant materials are important for extending operational lifetime of solar modules and maintaining their electrical performance over time by protecting solar cells from UV rays, moisture intrusion and mechanical stress. Polymer science plays an important role in this context. Next generation encapsulants are being evaluated and developed from polymers. Polymers like PBMA have become promising encapsulants because of their unique combination of mechanical strength, UV resistance, and excellent optical clarity [23].

The value of this research is not only in material optimization but also in its place in the bigger scheme of energy policy and climate change mitigation. Solar PV is an important piece of the puzzle in the United Nations' Sustainable Development Goal 7, which calls for modern, affordable, reliable and sustainable energy for all. The objective of this research is to search for an encapsulant that is cheaper and better than the conventional EVA by improving the service life and efficiency of PV systems to the reliability and economy of solar energy solutions**.**

MATERIALS AND METHODOLOGY

Material Synthesis and polymerization

Monomer Selection: The primary monomer used in the production of PBMA was butyl methacrylate (BMA). It was typically combined with other co-monomers (such as methyl methacrylate) to achieve the desired viscosity and mechanical properties. The monomer used to obtain polystyrene was styrene. The subsequent

ISSN No. 2454-6194 | DOI: 10.51584/IJRIAS |Volume XI Issue X October 2026

blends were obtained by mixing styrene and butyl methacrylate monomers in the ratio of (25/75) %, and (75/25) % before polymerization.

Polymerization Process: Butyl methacrylate, styrene and their further mixtures were polymerized using free radical polymerization which commonly begins by heat, light or chemical initiators. In this study, heat was used for the polymerization. The reaction produced long chain of PBMA, PS and their blends respectively.

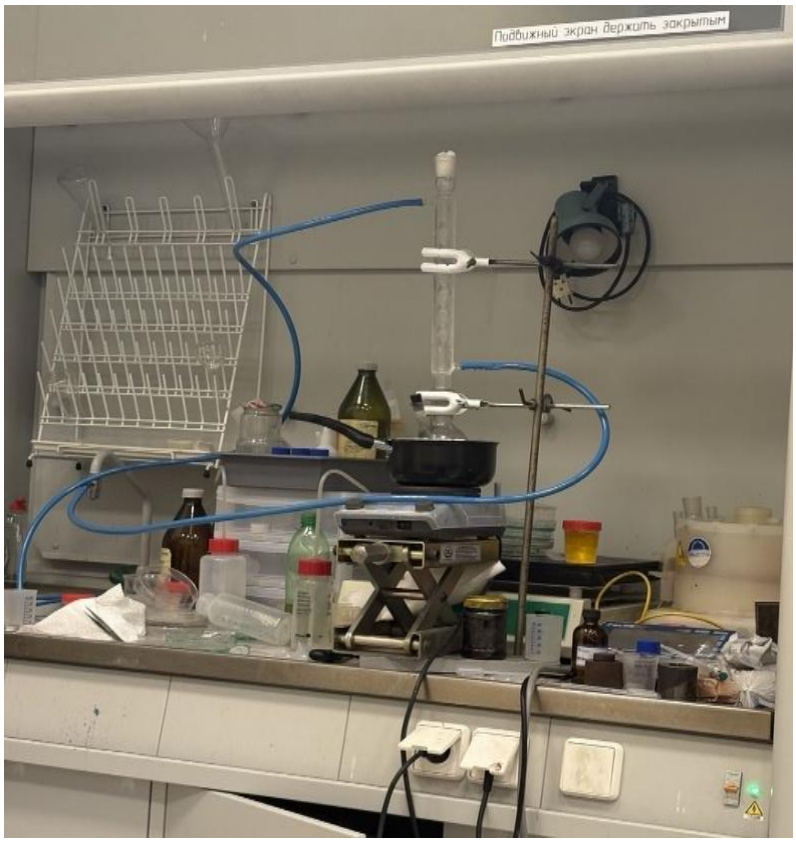


Fig. 1. Polymerization set up (Department of Material Science of Semiconductors and Dielectrics, MISIS)

Acetone was used as a solvent during the polymerization to help dissolve the monomers and control the viscosity of the resulting polymer. The degree of polymerization was controlled to achieve the desired molecular weight and viscosity which are essential for the processing and film formation required in solar cell encapsulation. The residual solvent used during the polymerization was evaporated under controlled conditions, using vacuum distillation. The samples were then purified to remove any residual monomers, solvents or impurities that could affect its performance as an encapsulant. The samples were filtered to remove any unreacted monomers or impurities, ensuring a clean polymer that will provide consistent performance in encapsulating applications

Processing and Casting: The solutions were transformed into a form appropriate for use as a solar module encapsulant. The polymeric solutions were cast into thin films to enclose the solar cell and glass substrates. They were cast by spin coating in order to get homogenous films with controlled thickness. The samples were cured with UV light to increase their mechanical strength and durability. This was done to achieve the desired hardness and adhesion properties. Transparency and optical clarity of the solutions are particularly important for the performance of the solutions as encapsulants. During the film-forming process, effort was made to minimize creation of bubbles or inclusions which could impair light transmission

Piranha Solution Based Cleaning for Glass Substrates: To allow for clean deposition of the polymerized solutions as encapsulant to the glass substrate, the glass surfaces were deeply cleaned with piranha solution. It was made by mixing H_2SO_5 and H_2O_2 (concentrated sulphuric acid and hydrogen peroxide) in 3:1 (volumetric ratio). This oxidative combination was used to remove organic materials and impurities from the surface of the substrate leaving a chemically active and hydrophilic surface

ISSN No. 2454-6194 | DOI: 10.51584/IJRIAS |Volume XI Issue X October 2026

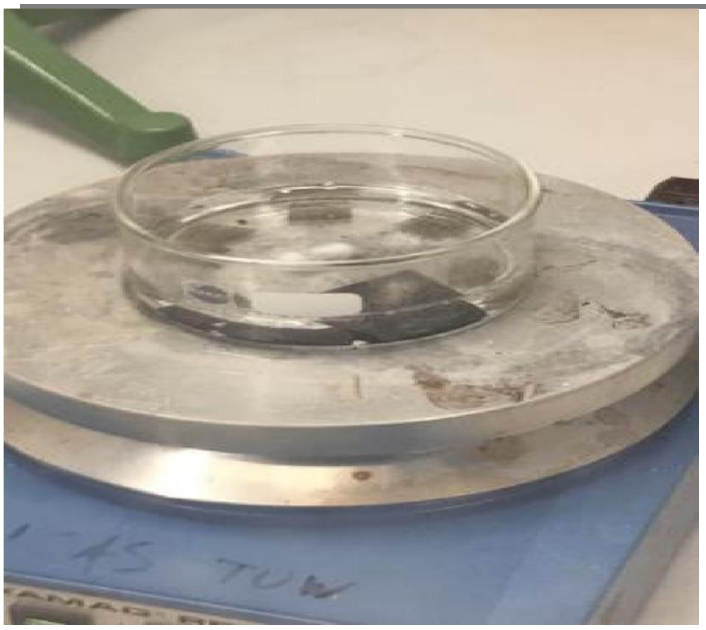


Fig. 2. The glass substrate placed in Piranha solution (Department of Material Science of Semiconductors and Dielectrics, MISIS University)

The cleaning process entailed soaking the glasses in newly made piranha solution for around 10 minutes at room temperature. After treatment, substrates were thoroughly washed with deionized water to remove residual acid and degradation by-products. The glasses were then dried using a stream of nitrogen gas in a clean and dust free environment to avoid recontamination. This process is very crucial to increase the surface wettability and to improve the interfacial bonding between the glass and polymer encapsulants. A clean, hydrophilic glass surface enables chemical and physical adhesion that eventually effects the efficacy of the encapsulants during mechanical testing and long term environmental exposure

Encapsulation Deposition: Following the careful cleaning of both glass and silicon substrates, the PBMA, PS and their subsequent blends in the ratio of (25/75 and 75/25)% encapsulants were applied on the substrates through a pipette which ensures a uniform and controlled film thickness necessary for PV module encapsulation

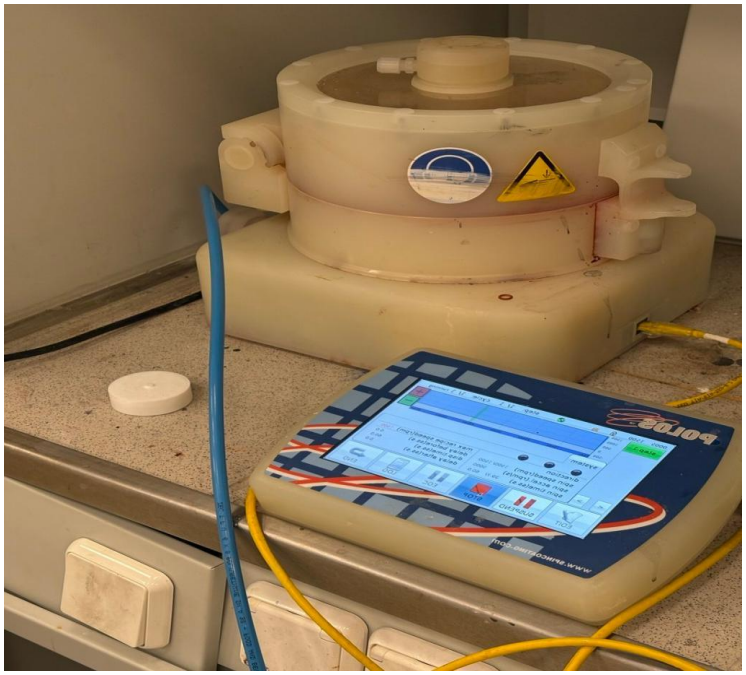


Fig. 3. Spin150i Spin Coater (Department of Material Science of Semiconductors and Dielectrics, MISIS)

The glass and silicon substrates were placed on a spin coater and the solutions were deposited onto the surfaces one by one. Each of the samples were spun at a specified rotational speed of 200 revolutions per minute (rpm) for a period of 60 seconds in a 150i spin coater. This process is allowed to generate a uniform, fault free encapsulant layer with a specified thickness needed to optimize the optical transparency and mechanical protection. The coated substrate were soft baked at moderate temperatures of 50,9^{o}C to remove residual solvents and enhance film adherence. It was then subjected to a further curing process at elevated temperatures of 70,9^{o}C for 15 minutes to increase the cross-linking of the polymers and to improve the mechanical toughness of the encapsulation. The polymers-glass substrates were stored in a dust free environment prior to further processing. This was done post-curing. All samples were prepared with great care and with utmost attention to consistency and uniformity in order to obtain reliable results during the testing process. The samples were sealed and stored in polyethylene bags in a climate controlled chamber to avoid any effect of climatic factors such as temperature and humidity. This guaranteed that the films were stable and protected from environmental stresses that could otherwise change their structure. The polymers on the different substrates were visually and microscopically inspected for absence of flaws such as bubbles and/or uneven edges that could compromise the overall performance as encapsulants

Adhesion Test

To measure the adhesion strength of the polymers as a solar cell encapsulant, a tape test was performed on both glass and silicon substrate correspondingly. This test is a straight forward and practical way to evaluate the polymer' superiority as encapsulants to glass and silicon substrate. This test is important to evaluate the mechanical performance of the encapsulants and their resistance to delamination and stress under normal operating conditions. The cross-hatch method was used. The number of blades and the spacing used was based on the thickness of the coating being evaluated.

The number of edges was 6 with a spacing of 1.0mm determined from the coating thickness for pure PBMA and (25/75)% respectively. For (75/25) % and pure PS the number of edges was 6 with a spacing of 3 mm.

Table 1 – Relevant standards for the cross-hatch method

No. of Edges	Spacing (mm)	Coating Thickness Range (µm)	Relevant Standard
11	1.0	0-50	ASTM only
6	1.0	0-60	ISO only
11	1.5	0-60	ASTM only
6	2.0	50-125	ASTM only
6	2.0	61-120	ISO only
6	3.0	125-250	ISO & ASTM

Adhesive properties of the polymers to the glass and silicon substrate were tested by a tape test. The tendency of delamination was determined by applying adhesive tape to the surface of the encapsulant and peeling it off

EVA Encapsulated on Glass Substrate

EVA granules were melted in an oven at 80^{o}C to generate a homogenous and consistent meltable polymer. This gave the right viscosity to make the ideal film. Then, the molten EVA was manually spread over the pre-cleaned glass substrates utilizing manual spreading techniques for even coating. The technique was closely monitored to ensure all samples were uniform in thickness of the EVA film. The substrates were then placed in a vacuum to cure the film at 80^{o}C for 15mins permitting cross-linking and ensuring that the EVA created a

ISSN No. 2454-6194 | DOI: 10.51584/IJRIAS |Volume XI Issue X October 2026

solid connection with the glass substrate. The cured glass EVA sample was allowed to cool down to room temperature and then stored in a dry cool place to avoid contamination.



Fig. 4. UT-4620 Vacuum Oven (Department of Material Science of Semiconductors and Dielectrics, MISIS)

Set up for UV-Induced Degradation Testing

An artificial UV degradation chamber was designed to simulate the real world conditions to which the solar cells and modules in general are subjected to. The setup followed viz;

A 25 watt UV-B light bulb was put in the middle of the chamber to ensure the samples were exposed uniformly. The light bulb emitted UV-B radiation in the wavelength range of 280-315nm, closely mimicking the UV radiation from the sun. This spectrum is the main reason for degradation of the polymers used for encapsulation in solar panels.

Ozone (O_3) is known to promote breakdown in polymers through oxidation, this UV-B bulb also emits this ozone portraying a real life scenario. The effect of ozone on the photo-oxidative degradation of polymers is studied to simulate the effect of the environment in the real outdoor circumstances of polymers. To increase UV exposure, reflective paper foils were attached to the outside walls of the UV chamber as shown in the image below. This was done to decrease direct UV exposure to the samples, and to raise the concentration of the UV radiation in the chamber by reflecting the light to the samples. The regulated environment allowed for equal exposure of both encapsulant ingredients. The temperature of the chambers was kept at 55^{o}C to imitate outdoor settings. Humidity was controlled at 50% to prevent undue influence of moisture on the samples. These environmental conditions were managed to ensure the consistency of the degradation process and to limit extraneous variables. All the samples were constantly exposed to UV light for a total of 365 hours. Daily exposure was carried out to ensure that the materials received an equivalent share of UV light across the whole trial period. All the samples were placed at similar distances from the UV-B light bulb and parallel to the light source. This artificial set up allowed both materials to be exposed to UV. Each sample was kept 20cm from the UV source to achieve similar radiation intensity

Raman Analysis

After the exposure period, all the encapsulated glass samples including that of EVA were carefully removed from the UV-chamber. Samples were cooled down to room temperature before any testing to avoid possible distortion due to thermal stress. The spectroscopic study was carried out using Raman spectrometer. The spectrometer was excited by a 532 nm laser. This wavelength was chosen because it could ignite the polymer

ISSN No. 2454-6194 | DOI: 10.51584/IJRIAS |Volume XI Issue X October 2026

efficiently and minimize the fluorescence interference. Raman spectra were measured on different points of the surface of each sample.

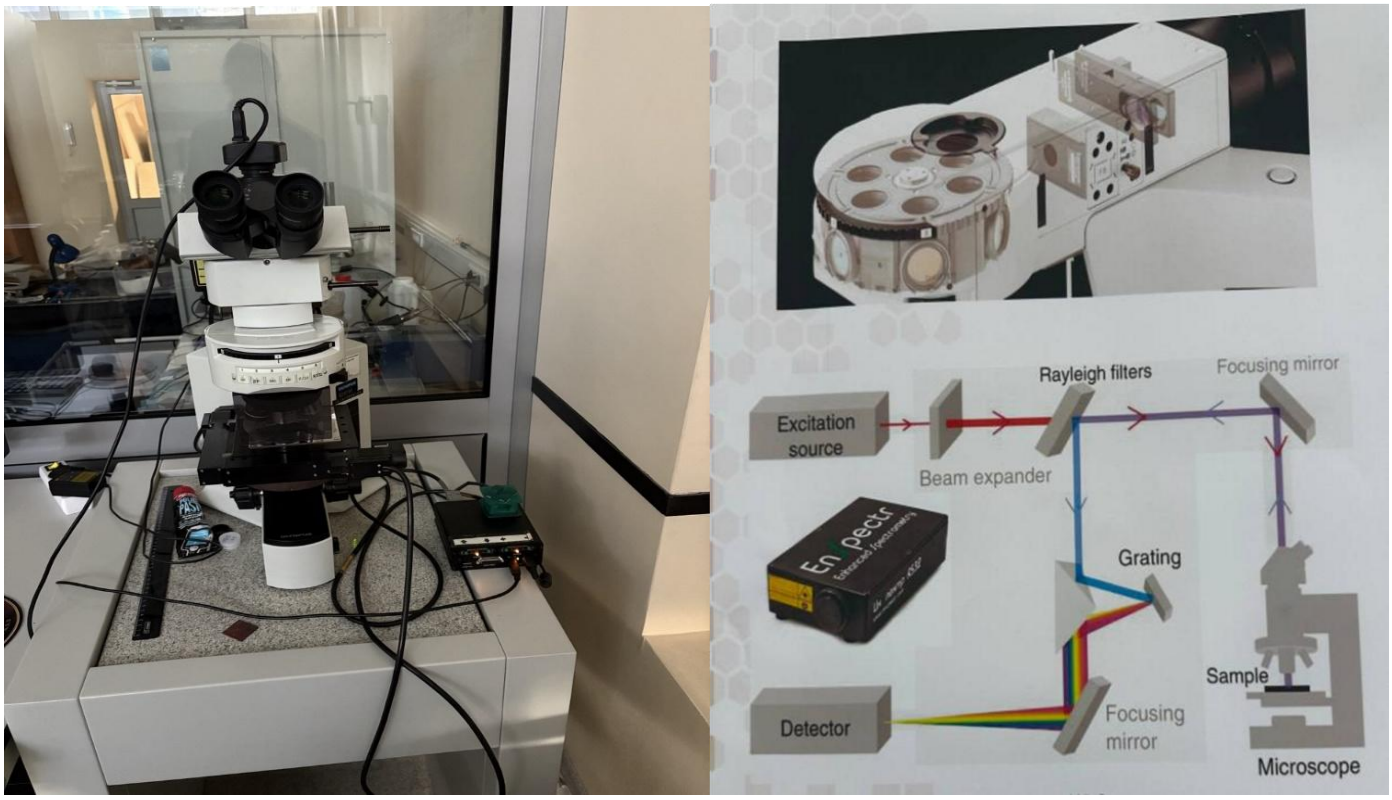


Fig. 5. Showing microscope embedded with Enspectra (Department of Material Science of Semiconductors and Dielectrics, MISIS)

The spectra were measured with an integration time of 10 seconds each measurement. Several scans were performed and averaged to minimize noise and improve resolution in order to improve quality. The equipment

was calibrated for precision to each measurement for accuracy. The chemical stability of the samples were evaluated using Raman spectroscopy to study the molecular structure before and after artificial UV ageing. Raman spectra were recorded and analyzed for distinctive peaks indicative of changes in the polymeric structure, specifically those associated with photo-oxidation owing to UV exposure. The Raman spectroscopy data gathered were searched for the breakage of polymer chains or production of degradation products. This was done by monitoring changes in the Raman peaks.

This investigation was done to compare two Raman Spectra which is; the one acquired before UV exposure and the other after exposure for 365 hours. The idea is to test molecular changes of polymers due to degrading impacts of UV light and aid to evaluate its appropriateness as a long-term encapsulant in solar applications. Spectroscopy measurements were conducted on an Enspectr R532 Raman spectrometer with a 532 nm source. Spectra of each polymer were recorded under standard settings so as to assure reproducibility of the results.

Moisture Absorption Test

This test is required to determine the measure of how much moisture the encapsulant polymer material can absorb which is critical for determining dimensional stability and mechanical performance. The samples were spin coated on a glass substrate after been washed with piranha solution using spin150i coater for 200rpm to ensure a uniform deposition. The samples were then dried in a UT-460 oven to remove existing moisture at 50^{o}C. Prior to the deposition of the samples, the glasses were weighed and their masses determined. The masses of the samples + glasses were determined before and after immersion in water after 24 hours. The percentage of water absorption of the polymers was determined by $\frac{W2-W1}{W1}.100$

ISSN No. 2454-6194 | DOI: 10.51584/IJRIAS |Volume XI Issue X October 2026

RESULTS

Adhesion Test Evaluation

Observation from the adhesion test using the minimal removal of the encapsulant was made which indicated strong adhesion for pure PBMA and blends in the ratio of (25/75 & 75/25) % respectively. Pure polystyrene was observed to have relative low adhesion properties when compared to the above mentioned polymers.

Table 2 – the adhesion test result of the samples

Sample	Classification	No. of Removal
Pure PBMA	5B	0
25/75%	5B	0
75/25%	4B	1
Pure PS	3B	2

From the tape test carried out as reported in Table 2, 5B classification was achieved for pure PBMA and (25/75) % blend solutions. On the other hand, a 4B classification with one removal was achieved for (75/25) % blend sample. A 3B classification was reportedly observed with pure polystyrene. The quantity and pattern of removal are useful in assessing the quality of adhesion.

The first 3 samples showed no or very little loss of the coatings indicating good adherence. Except for pure polystyrene, the tape showed some visible particles and residue related to the coating and the surface layer of the substrate. This confirms that part of the substance of the polymer peeled off during testing. In the case of pure PBMA and the (25/75) % blend polymer solutions, no coating was evident on the tape and no coating was absent from the substrate which corresponds to a satisfactory adhesion rating which is 5B in ASTM and 0 in

ISO. For (75/25) % blends a small quantity of coating was seen on the tape and not on the substrate which is equivalent to a satisfactory adhesion rating assessed as 4B in ASTM and rating 1 in ISO.

Moisture Test Analysis

Moisture test is done to measure the amount of water a material (polymer) absorbs or allows to pass through, usually measured by weight gain, gravimetric analysis or for components and electrical leakage.

Table 3 – moisture absorption test outcome

Glass (g)	Glass + Polymer Before Immersion(g)	Polymer before immersion W_1(	Glass + Polymer After Immersion (g)	Polymer After Immersion W_2 (g)	Weight percentage (%)
5.033	Glass + PBMA = 5.048	0.015	Glass + PBMA =5.048	0.015	0
5.038	Glass + PS = 5.054	0.016	Glass + PS = 5.054	0.016	0
4.89	Glass + (25/75) = 4.901	0.011	Glass + (25/75) = 4.902	0.012	0.02
5.155	Glass + (75/25) = 5.169	0.014	Glass + (75/25) = 5.169	0.014	0

Table 3 shows that PBMA had zero tolerance to water absorption after 24 hours of immersion. Pure PS recorded 0%wt, likewise the (75/25) % blend. (25/75) % blend experienced a 0.020% water absorption. The allowable acceptable water absorption for encapsulation materials for solar cells is less than 0.5wt%. The polymers under study demonstrated to be excellent materials for solar cell encapsulation.

ISSN No. 2454-6194 | DOI: 10.51584/IJRIAS |Volume XI Issue X October 2026

Raman Spectroscopy and Aging Test Analysis for PBMA

As illustrated in fig. 6, the black spectrum correspond to PBMA film in its native condition whereas the red spectrum illustrates the structural state of the same polymer following UV ageing.

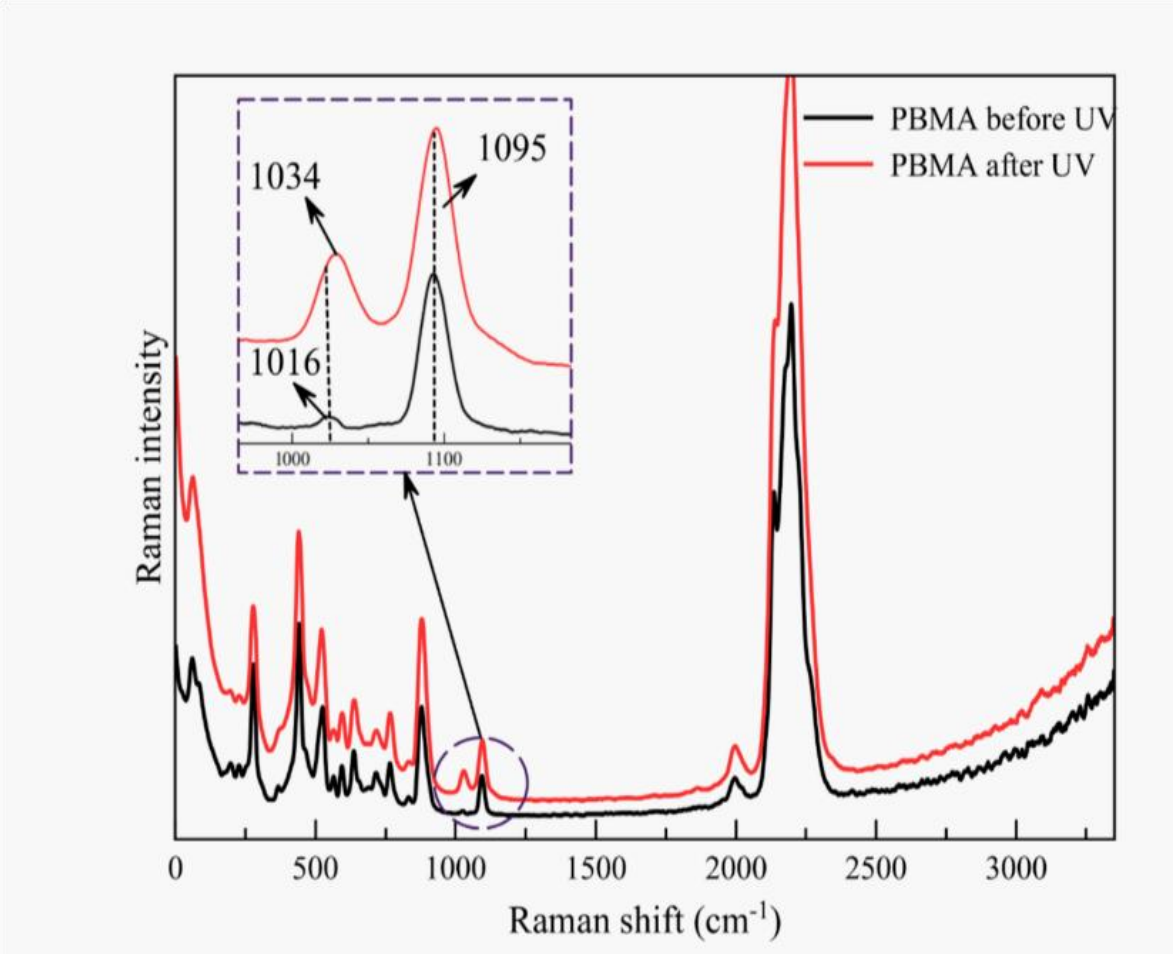


Fig. 6 Comparison of PBMA Raman Spectral Before and After 364 Hours of UV-B Exposure

At 1016 cm^{-1} PBMA exhibited a strong peak ascribed to C-C stretching and C-O bending characteristic of the methacrylate backbone. An oxidized free polymeric structure is observed in the 1030-1100 cm^{-1} region due to the absence of high intensity peaks.

A more expanded view of the (1000-1120) cm^{-1} region is also shown to allow close investigation of any forming peaks. Visible alterations of the Raman spectrum of PBMA were seen in the (1000-1120) cm^{-1} area after 364 hours of UV exposure. The original 1016 cm^{-1} peak underwent a shift and lowered relative intensity and a new peak appeared at 1034 cm^{-1}. This development of new peaks is attributed to photo-oxidative alterati-

ons in the polymer chain probably due to the formation of peroxide species, oxidized C-O-C linkages or conjugated side chain structures due to UV-induced chain scission or cross linking processes [16]. Furthermore, the Raman intensity in the (400-1800) cm^{-1} range increased following the UV treatment. This suggests greater molecular disarray or the introduction of new oxidation-related vibrational modes. However, the aliphatic hydrocarbon framework of PBMA preserved mainly its structural integrity as evidenced by the still prominent acute and dominating C-H stretching peak about 29540 cm^{-1} in both samples.

These Raman spectra suggest that PBMA exhibits photo-oxidative alterations under long term UV exposure. However the extent of degradation is moderate and essentially limited to the side chain and the ester part of the molecules. This observation is in agreement with the projected UV resistance of PBMA and further supports its prospective appropriateness and implementation as a viable and durable encapsulant.

Raman Spectroscopy and Aging Test Analysis for (25/75) % Blend

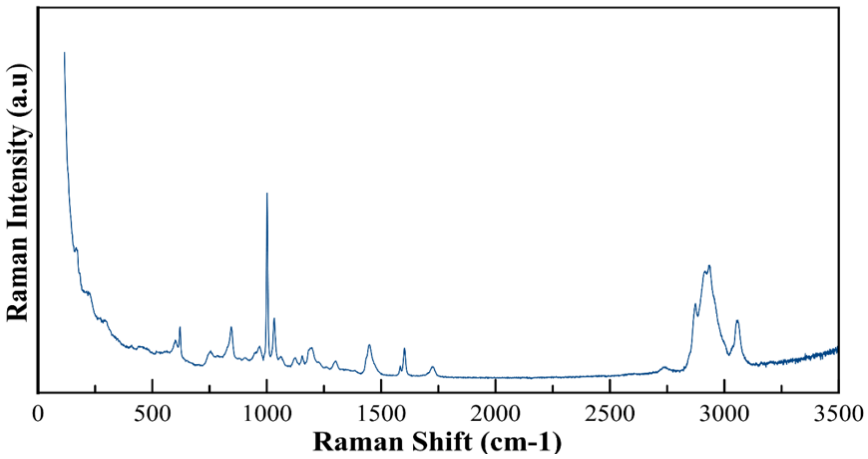


Fig. 7. Comparison of (25/75) % blend Raman Spectral Before and After 252 Hours of UV-B Exposure

Raman spectrum revealed distinct characteristics peaks for both PS and PBMA despite the fact that the blend is PBMA dominant with 75%. A strong peak is observed at 1000 cm^{-1} (a phenyl breathing mode of polystyrene). This confirms that PS is well dispersed even at 25%. Another peak is noticed at 1600 cm^{-1} indicating an aromatic C=C stretching, also indicating the presence of PS. At 1720 cm^{-1} a peak is also observed which indicate a carbonyl (C=O) stretching of PBMA. This peak is not obviously visible suggesting a weak Raman activity of carbonyl or overlap with other features probably that of Polystyrene. A peak appeared at 1450 cm^{-1} showing the presence of a CH_2 bending which is indicative of both PS and PBMA. Aliphatic and Aromatic C-H stretches are observed at the (2800-3100) cm^{-1} peak. The strong PS signal at 1000 cm^{-1} dominating the spectrum despite lower concentration indicates that PS has a much higher Raman scattering cross-section than PBMA which is due to the aromatic ring.

After 252 hours of UV-B exposure, no noticeable new peaks were seen, indicating the absence of photo-oxidation products. This underscores a good photo-stability of the blend which is unusual of polymers containing polystyrene. The high PBMA content of 75 % likely protects PS through diluent effects or energy transfer mechanisms. The PS/PBMA (25/75) % blend demonstrated remarkable photochemical stability under 252 hours of UV exposure with Raman spectroscopy revealing no noticeable chemical degradation which positions the polymer blend as potential encapsulant for solar modules.

Raman Spectroscopy and Aging Test Analysis for (75/25) % Blend

It was observed that the Raman spectrum of the (75/25) % blend of Polystyrene (PS) and Poly-Butyl Methacrylate (PBMA) revealed the characteristics bands from both components with PS dominating due to its higher concentration and its intrinsically stronger Raman scattering. The peak at 1000 cm^{-1} is the most visible feature. The weak PBMA carbonyl Raman peak which appears near 1725 cm^{-1} could be as a result of being submerged under PS background.

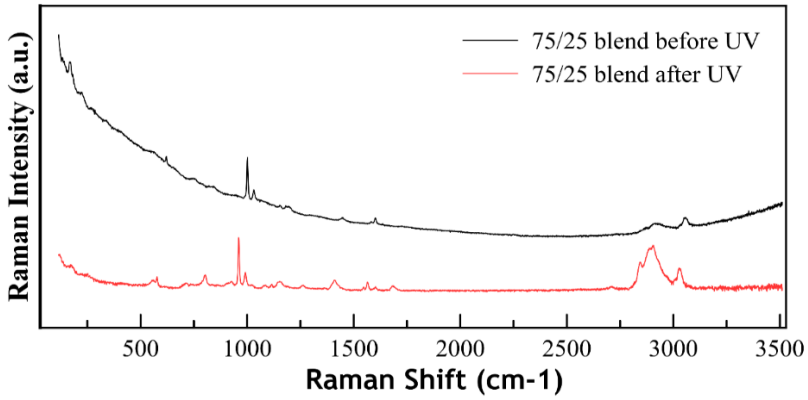


Fig. 8. Comparison of (75/25) % Blend's Raman spectral before and after 230 Hours of UV-B exposure

ISSN No. 2454-6194 | DOI: 10.51584/IJRIAS |Volume XI Issue X October 2026

Fig. 8 shows the Raman Spectra of (75/25) % blend before and after 230 hours of UV-B exposure. The characteristics peaks of Polystyrene especially the visible ring breathing mode at 1000 cm^{-1} and the aromatic C=C stretch at 1600 cm^{-1} remain almost in the same position and intensity. The weak carbonyl stretch of PBMA near 1725 cm^{-1} shows no significant shift or broadening. The absence of new peaks in the (3200-3500) cm^{-1} (O-H) or (1700-1800) cm^{-1} (C=O) regions indicates that little or no photo-oxidation nor chain scission occurred. The stability suggests that even at 75% PS loading, the PBMA component doused down the excited states of PS.

Raman Spectroscopy and Aging Test Analysis for Polystyrene (PS)

Fig. 9 is an illustration of Raman spectra for pure polystyrene before and after 230 hours of UV-B irradiation exposure which simulates real world UV radiation. Before aging, the spectrum showed the characteristics sharp ring breathing mode at 1000 cm^{-1} and the aromatic C=C stretching doublet near 1585 to 1602 cm^{-1} which confirms that the phenyl rings are intact. After UV-B exposure, the intensity of the 1000 cm^{-1} band decreases notably, accompanied by peak broadening and a rising baseline which indicate the presence of fluorescence from conjugated degradation products. Most critically, a new broad feature appears near 1600 cm^{-1} which is assigned to carbonyl (C=O) stretching vibrations from photo-oxidized chain ends. These spectral changes demonstrate that pure polystyrene undergoes severe photo degradation under UV-B conditions with both chain scission and ring oxidation occurring concurrently.

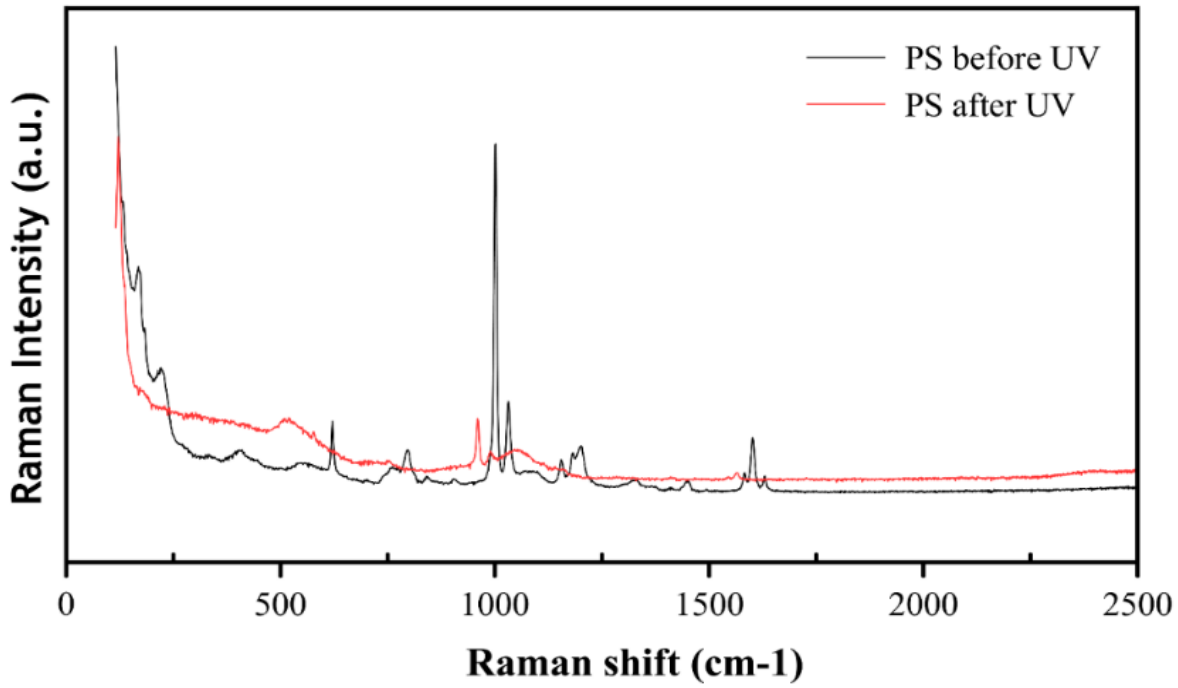


Fig. 9. - Comparison of PS Raman spectral before and after 230 hours of UV-B exposure

Consequently, pure polystyrene fails to meet the strict stringent long term stability requirements for solar cell encapsulation. The degradation mechanism in pure polystyrene likely proceeds through Norrish type II abstraction followed by β-scission which generates carbonyl moieties and conjugated polyenes which is responsible for yellowing.

Raman Spectroscopy and Aging Test Analysis for EVA

Raman spectroscopy was deployed to monitor molecular structure of EVA before and after UV-B irradiation to evaluate its photochemical stability. In the image below (figure 10), the black curve is the profile of the EVA vibrational before the UV exposure and the red curve is the profile of the EVA vibrational after 292 hours of continuous UV exposure in the artificial UV chamber . The inner graph illustrates the (1000 – 1120) cm^{-1} region where major structural alterations were observed. It formed a

ISSN No. 2454-6194 | DOI: 10.51584/IJRIAS |Volume XI Issue X October 2026

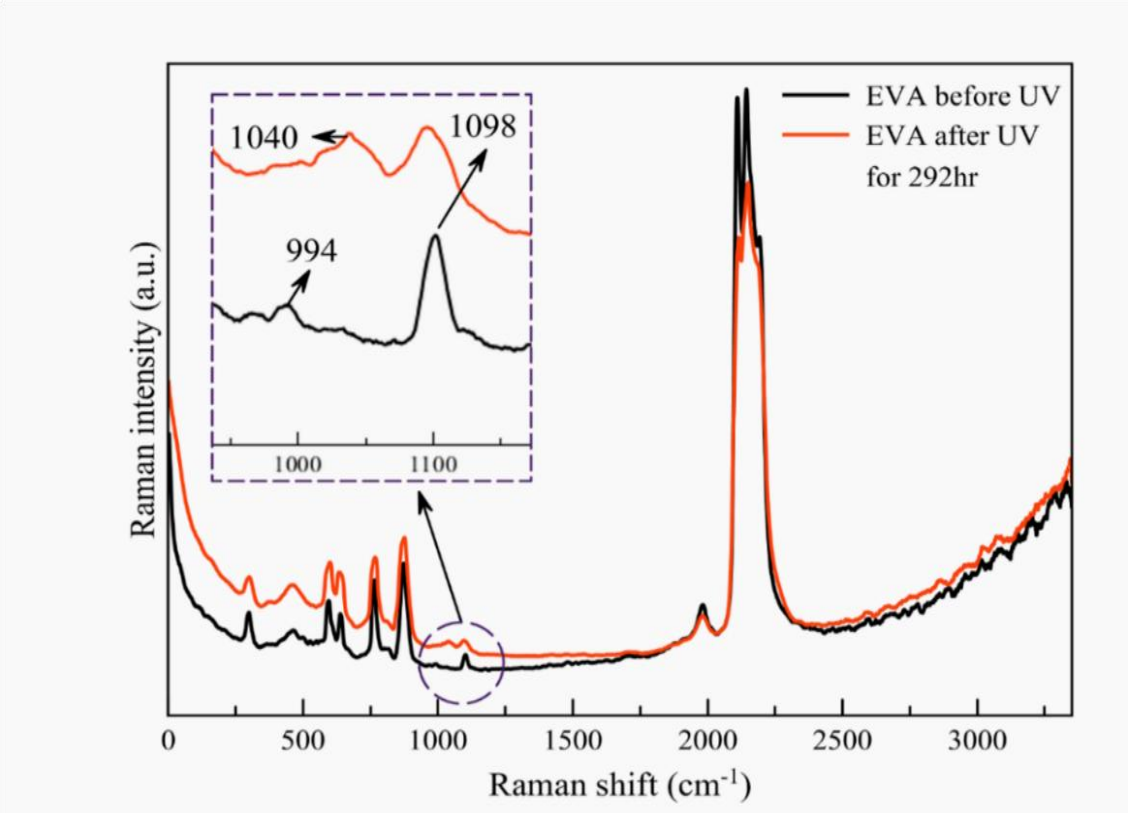


Fig. 10. Comparison of EVA Raman spectral before and after 292 hours of UV-B exposure

Distinct peak in the 994 cm^{-1} area corresponding to C-C stretching and C-H deformation modes which are indicative of a stable polyethylene/vinyl acetate backbone. The lack of subsequent strong peaks and the low intensity baseline in this region support the initial integrity of the molecule of the polymer.

After 292 hours of continuous UV exposure, a new peak appeared at 1040 cm^{-1} replacing the initial 994 cm^{-1} band with larger and higher intensity signals. Such alterations are characteristic of photochemical oxidation due to long-term UV exposure. This points to a breaking of the integrity of the chain in the sense of oxidative degradation and crosslinking. Especially in the low wavenumber range (<800 cm^{-1}) an increase of the Raman background intensity indicating structural disorder and non-crystalline by-products such as polyene sequence was detected. The polyethylene backbone maintained its structural integrity, even though the side chain functional groups and vinyl acetate groups were affected, evidenced by the relatively stable high C-H stretching peak at 2950 cm^{-1} in the sample (pre and post exposure spectra) despite significant chemical changes.

The emergence of novel vibrational characteristics after 292 hours of UV exposure reveals that EVA undergoes significant photo-oxidative deterioration during simulated solar ageing, with implications for the durability of EVA. New peaks related to the breakdown of vinyl acetate units are a well-known degradation process in EVA used for solar module encapsulation.

Comparative Analysis of PBMA, PS and the blends against EVA after UV Exposure

Comparative Spectral Changes

Table 4 – Summary of the main spectral features observed for all polymers before and after UV exposure.

Polymer	**Time for UV Exposure**	**Peak Before UV (cm^{-1})**	**New Peak After UV (cm^{-1})**	**Inference**
EVA	292	994	1040	Vinyl oxidation, C-O-O ether linkages
PBMA	364	1016	1034	C-O Stretching and oxidative bond formation

PS	230	1000	960, 1602	Carbonyl (C=O) stretching vibrations from photo-oxidized chain.
(25/75)% blend	252	1450	No visible peak	Little or no serious photo-oxidation
(75/25)% blend	230	1000	960	Presence of oxidation

The presence of new peaks in all the samples except (25/75) % blend is evidence for the creation of oxidized functional groups and is generally related with photo-induced chain scission and crosslinking reactions. These changes influence the optical transparency and the mechanical stability of the encapsulants over time. However, the time and extent of such degradations are polymer specific. The (25/75) % blend and PBMA are less susceptible to UV-induced deterioration with less change in chemical composition. EVA exhibits fast photochemical reactions, which may jeopardize its long term use. The variations observed in the evolution of the peaks and spectrum shifts indicate the importance of the selection of the encapsulant not only based on their initial qualities but also on their photo-stability and chemical resilience under the simulated ageing conditions.

Evaluation of Optical Performance for PBMA and EVA

Table 5 – Comparison of PBMA to EVA transmittance

Wavelength	*PBMA*	*EVA*	*Wavelength*	*PBMA*	*EVA*
2500	71.2124	37.8087	2485	71.09339	33.7094
2499	71.2198	37.6939	2484	71.08698	33.4004
2498	71.2316	37.5575	2483	71.07323	33.0882
2497	71.2297	37.3956	2482	71.0621	32.7977
2496	71.2202	37.1927	2481	71.04216	32.523
2495	71.2094	36.956	2480	71.03954	32.2738
2494	71.214	36.7039	2479	71.03223	32.0284
2493	71.1899	36.4172	2478	71.01529	31.8132
2492	71.1789	36.12	2477	71.00566	31.6018
2491	71.1686	35.7958	2476	71.00556	31.4053
2490	71.1583	35.4546	2475	71.00433	31.2231
2489	71.1568	35.0957	2474	70.99562	31.0627
2488	71.1221	34.7283	2473	70.98426	30.8853
2487	71.1303	34.3962	2472	70.96381	30.7148
2486	71.1088	34.0502			

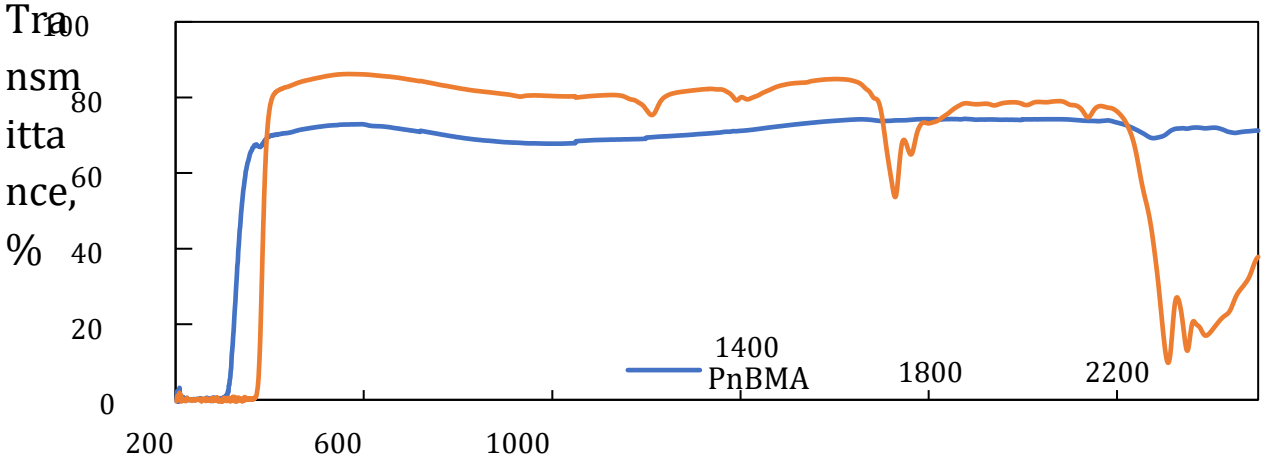


Fig. 11. Chart showing PBMA and EVA across a range of wavelengths

ISSN No. 2454-6194 | DOI: 10.51584/IJRIAS |Volume XI Issue X October 2026

Fig 11 shows the transmittance spectra of both materials across a wavelength range of (200-2400) cm^{-1} showing clear distinctions in their optical transmittance and spectral consistency. The vertical axis shows the percentage of light transmitted through the polymer film, while the horizontal axis denotes the wavenumber in (cm^{-1}) aligning with the incident light wavelengths.

Comparison of Optical Transmittance of PBMA and EVA

From fig. 11, PBMA which is represented by the blue curve showed average transmittance ranging from (65-75) % with a stable spectral profile. The reduced intensity suggests higher intrinsic absorption or thicker film application but also indicates greater spectral consistency across the mid – IR region. More importantly, PBMA did not exhibit the sharp absorption valleys seen in EVA which is indicative of a more optical uniform structure with little active impurities or degradation prone sites.

On the other hand, EVA represented by the orange curve demonstrated high transmittance across the visible and near infrared range consistently reaching values above 85 % between approximately 500 cm^{-1} to 1700 cm^{-1}. Multiple sharp dips were seen, particularly near 1750 cm^{-1} and a significant drop around 2200 cm^{-1}, indicating selective absorption or interference due to residual additives, internal reflection or degradation by products. EVA maintained excellent average transmittance in the active photovoltaic spectral range despite the fluctuations. This is a key factor for its massive adoption.

From fig. 12, EVA shows stronger transmittance with 88 % in the visible range of (400 -700) cm^{-1} whereas PBMA transmitted about 70 % showing a slight low optical transmittance but still within allowable limits for photovoltaic encapsulation. Near infrared region of (700-1400) cm^{-1}, EVA showed higher transmission of 86 % which is still higher than that of PBMA which is 72 %. EVA drops to 82 % in the

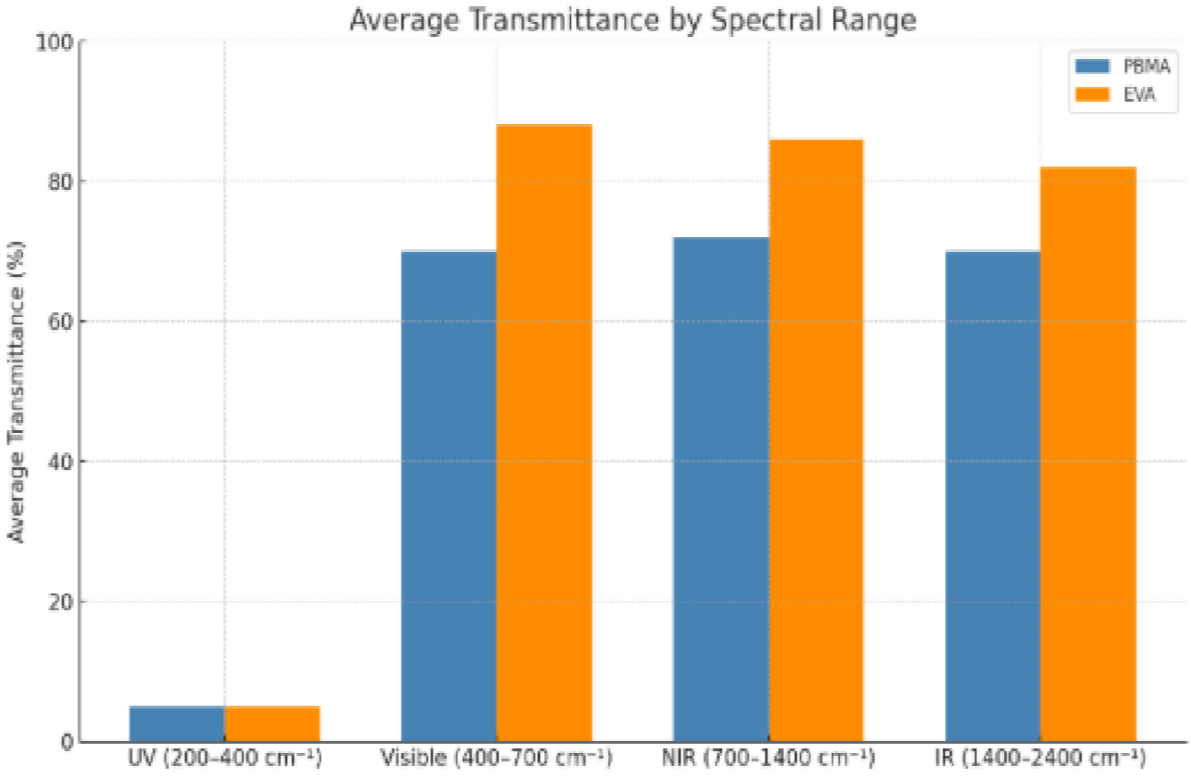


Fig. 12. Average Transmittance by Spectral Range for PBMA and EVA

Infrared region of (1400-2400) cm^{-1} while PBMA maintained its stability of 70 % indicating EVA's spectral vulnerability to absorption dips observed in the transmittance curve. Both EVA and PBMA show weak transmission of barely 5%, which is good for UV blocking to protect underlying solar cell layers. The graph in fig. 12 further substantiate the Raman analysis which says PBMA provides more stable spectral and smoother performance while EVA presents higher peak transparency but has high spectral instability.

ISSN No. 2454-6194 | DOI: 10.51584/IJRIAS |Volume XI Issue X October 2026

CONCLUSION

The overall evaluation of these polymers (excluding pure Polystyrene) as encapsulant material for solar modules has shown significant potential to overcome the obstacles posed by conventional encapsulants. The PBMA and the mixes showed a balanced combination of optical transparency, mechanical resilience and chemical stability which are the important parameters for long-term solar cell protection following stringent mechanical, chemical and optical testing. Raman spectroscopy analysis demonstrated the stability of PBMA, (25/75) % and (75/25) % during rapid ultraviolet exposure, with little or restricted photo-oxidative degradation and preservation of molecular integrity. The tape testing after standard compliance substrate cleaning processes demonstrated the polymers' good adhesive capabilities and resistance to delamination which are crucial for sustaining module stability under high environmental stress.

Optical transmission experiments confirmed that PBMA is able to maintain outstanding levels of light transmittance along the solar spectrum, resulting in negligible optical losses and so supporting continuous photovoltaic efficiency. These properties suggest that PBMA can increase the operational lifetime of solar modules by preventing common degradation mechanisms related to moisture ingress, UV damage and mechanical stress.

The addition of PBMA and the mixes to photovoltaic production processes offers a viable route towards more durable, efficient, and cost-effective solar energy systems. These discoveries provide a strong basis for further research and development targeted at optimizing polymer formulations and processing techniques to fully harness the polymers' benefits in commercial solar cell applications.

REFRENCES

1. Allen, N. S., et al. (2000). Aspects of the thermal oxidation, yellowing and stabilization of ethylene vinyl acetate copolymer. *Polymer Degradation and Stability, 71*(1), 1–14.
2. Barretta, C., Macher, A. E., Ascencio-Vásquez, J., et al. (2022). Degradation of crystalline silicon photovoltaic modules installed in different climates. In *Proceedings of the IEEE 49th Photovoltaic Specialists Conference (PVSC)* (pp. 680–682). IEEE.
3. Carlson, D. E., Romero, R., Willing, F., Meakin, D., Gonzalez, L., Murphy, R., Moutinho, H. R., & Al-Jassim, M. (2003). Corrosion effects in thin-film photovoltaic modules. *Progress in Photovoltaics: Research and Applications, 11*(6), 377–386. https://doi.org/10.1002/pip.500
4. Charki, A., Laronde, R., & Bigaud, D. (2012). The time-variant degradation of a photovoltaic system. *Journal of Solar Energy Engineering, 135*(2).
5. Daher, D. H., Gaillard, L., & Ménézo, C. (2022). Experimental assessment of long-term performance degradation for a PV power plant operating in a desert maritime climate. *Renewable Energy, 187*, 44–55.
6. Dhimish, M., & Tyrrell, A. M. (2022). Power loss and hotspot analysis for photovoltaic modules affected by potential induced degradation. *npj Materials Degradation, 6*, Article 11. https://doi.org/10.1038/s41529-022-00221-9
7. de Oliveira, D. C. B. (2018). The causes and effects of degradation of encapsulant ethylene vinyl acetate copolymer (EVA) in crystalline silicon photovoltaic modules: A review. *Renewable and Sustainable Energy Reviews, 81*, 2299–2317.
8. Hara, K., Jonai, S., & Masuda, A. (2015). Crystalline Si photovoltaic modules functionalized by a thin polyethylene film against potential and damp-heat-induced degradation. *RSC Advances, 5*(20), 15017–15023.
9. Heidrich, R., Mordvinkin, A., & Gottschalg, R. (2023). Spatially resolved degradation analysis of solar modules after combined accelerated aging. In *Proceedings of the IEEE 50th Photovoltaic Specialists Conference (PVSC)* (pp. 1–3). IEEE.
10. Jansen, K. W., & Delahoy, A. E. (2003). A laboratory technique for the evaluation of electrochemical transparent conductive oxide delamination from glass substrates. *Thin Solid Films, 423*, 153–160.
11. Jha, V. (2023). Generalized modelling of PV module and different PV array configurations under partial shading condition. *Sustainable Energy Technologies and Assessments, 56*.

12. Jin, J., Chen, S., & Zhang, J. (2010). UV aging behaviour of ethylene-vinyl acetate copolymers (EVA) with different vinyl acetate contents. *Polymer Degradation and Stability, 95*(5), 725–732.
13. Kempe, M. D. (2005). Control of moisture ingress into photovoltaic modules. In *Proceedings of the 31st IEEE Photovoltaic Specialists Conference*. IEEE.
14. Kempe, M. D. (2006). Modelling the moisture ingress into photovoltaic modules. *Solar Energy Materials and Solar Cells, 90*, 2720–2738.
15. Kempe, M. D. (2010). Ultraviolet test and evaluation methods for encapsulants of photovoltaic modules. *Solar Energy Materials and Solar Cells, 94*, 246–253.
16. Kim, J., Rabelo, M., Padi, S. P., et al. (2021). A review of the degradation of photovoltaic modules for life expectancy. *Energies, 14*(14), Article 4278.
17. Kojima, T., & Yanagisawa, T. (2004). The evaluation of accelerated test for degradation of a stacked a-Si solar cell and EVA films. *Solar Energy Materials and Solar Cells, 81*(1), 119–123.
18. Ndiaye, A., Charki, A., Kobi, A., et al. (2013). Degradations of silicon photovoltaic modules: A literature review. *Solar Energy, 96*, 140–151.
19. Oreski, G., Omazic, A., Eder, G. C., Voronko, Y., Neumaier, L., Mühleisen, W., Hirschl, C., Ujvari, G., Ebner, R., & Edler, M. (2020). Properties and degradation behaviour of polyolefin encapsulants for photovoltaic modules. *Progress in Photovoltaics: Research and Applications, 28*(12), 1277–1288. https://doi.org/10.1002/pip.3323
20. Oreski, G., & Wallner, G. M. (2005). Aging mechanisms of polymeric films for PV encapsulation. *Solar Energy, 79*, 612–617.
21. Oreski, G., & Wallner, G. M. (2009). Evaluation of the aging behavior of ethylene copolymer films for solar applications under accelerated weathering conditions. *Solar Energy, 83*, 1040–1047.
22. Osterwald, C. R., Anderberg, A., Rummel, S., & Ottoson, L. (2002). Degradation analysis of weathered crystalline-silicon PV modules. In *Proceedings of the 29th IEEE Photovoltaic Specialists Conference*. IEEE.
23. Osterwald, C. R., & McMahon, T. J. (2009). History of accelerated and qualification testing of terrestrial photovoltaic modules: A literature review. *Progress in Photovoltaics: Research and Applications, 17*(1), 11–33. https://doi.org/10.1002/pip.861
24. Patel, M., et al. (2013). Thermal stability of poly(ethylene-co-vinyl acetate) based materials. *Polymer Testing, 32*(4), 785–793.
25. Rimez, B., et al. (2008). The thermal degradation of poly(vinyl acetate) and poly(ethylene-co-vinyl acetate), Part II: Modelling the degradation kinetics. *Polymer Degradation and Stability, 93*(6), 1222–1230.
26. Shaik, F., Lingala, S. S., & Veeraboina, P. (2023). Effect of various parameters on the performance of solar PV power plant: A review and experimental study. *Sustainable Energy Research, 10*(1), Article 6. https://doi.org/10.1186/s40807-023-00076-x
27. Vázquez, M., & Rey-Stolle, I. (2008). Photovoltaic module reliability model based on field degradation studies. *Progress in Photovoltaics: Research and Applications, 16*(5), 419–433. https://doi.org/10.1002/pip.825
28. Wang, H., Cheng, X., & Veeraboina, P. (2019). Potential-induced degradation: Recombination behavior, temperature coefficients and mismatch losses in crystalline silicon photovoltaic power plant. *Solar Energy, 188*, 258–264.
29. Wohlgemuth, J. H., & Kurtz, S. (2011). Reliability testing beyond qualification as a key component in photovoltaics' progress toward grid parity. In *Proceedings of the IEEE International Reliability Physics Symposium*. IEEE.
30. Yang, W., Zhang, Y., Xiao, C., et al. (2025). A review of encapsulation methods and geometric improvements of perovskite solar cells and modules for mass production and commercialization. *Nano Materials Science*.
31. IEA-PVPS, "Snapshot 2025 Report." [Online]. Available: *IEA-PVPS.org/Snapshot-reports/snapshot-2025*